

System Level Evaluation of Network-Controlled Repeaters: Performance Improvement of Serving Cell and Interference Impact on Neighbor Cells

Gabriel C. M. da Silva, Erik R. B. Falcão, Victor F. Monteiro, Darlan C. Moreira, Diego A. Sousa, Tarcisio F. Maciel, Fco. Rafael M. Lima and Behrooz Makki.

Abstract—Heterogeneous networks have been studied as one of the enablers of network densification. These studies have been intensified to overcome some drawbacks related to propagation in millimeter waves (mmWaves), such as severe path and penetration losses. One of the promising heterogeneous nodes is network-controlled repeater (NCR). It was proposed by the 3rd generation partnership project (3GPP) in Release 18 as a candidate solution to enhance network coverage. In this context, this work performs a system level evaluation to analyze the performance improvement that an NCR can cause in its serving cell as well as its interference impact on neighbor cells. Particularly, the results show a considerable improvement on the performance of user equipments (UEs) served by the NCR, while neighbor UEs that receive the NCR signal as interference are negatively impacted, but not enough to suffer from outage.

Index Terms—network-controlled repeater (NCR), wireless backhaul, coverage, fifth generation (5G), sixth generation (6G).

I. INTRODUCTION

Compared to the previous generation of wireless cellular systems, fifth generation (5G) networks have explored higher frequencies, e.g., millimeter waves (mmWaves) [1]. Some of the reasons for this interest are the fact that in mmWaves there are larger portions of available spectrum and that the required antenna arrays are smaller, which allows the deployment of more antenna elements creating narrow beams with high directional gain [1]–[3]. Nonetheless, there are some disadvantages, e.g., suffering from high path and penetration losses [2], [4].

One of the considered solutions to overcome the propagation losses is network densification. However, building from scratch a completely new wired infrastructure is expensive, takes time and, in some places, trenching may not be allowed, like historical areas. Then, nodes with wireless backhaul have emerged as a possible solution for the situations where wired backhaul is not a viable solution [3], [5].

In this context, the present paper focuses on a new node with wireless backhaul called network-controlled repeater

Behrooz Makki is with Ericsson Research, Sweden. The other authors are with the Wireless Telecommunications Research Group (GTEL), Federal University of Ceará (UFC), Fortaleza, Ceará, Brazil. Diego A. Sousa is also with Federal Institute of Education, Science, and Technology of Ceará (IFCE), Paracuru, Brazil. This work was supported by Ericsson Research, Sweden, and Ericsson Innovation Center, Brazil, under UFC.51 Technical Cooperation Contract Ericsson/UFC. The work of Victor F. Monteiro was supported by CNPq under Grant 308267/2022-2. The work of Tarcisio F. Maciel was supported by CNPq under Grant 312471/2021-1. The work of Francisco R. M. Lima was supported by FUNCAP (edital BPI) under Grant BP4-0172-00245.01.00/20.

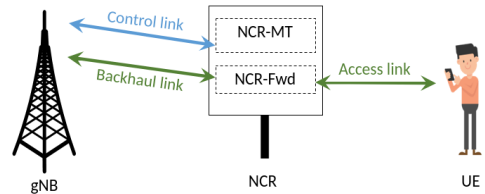


Fig. 1. NCR split in NCR-MT and NCR-Fwd.

(NCR) [6]. NCR was introduced by 3rd generation partnership project (3GPP) in Release 18 [7]. It is an enhanced version of traditional radio frequency (RF) repeaters. One of the novelties of NCRs is the fact that they have beamforming capability that can be controlled by a gNodeB (gNB) via side control information to improve the communication.

In this paper, we introduce the concept of NCR and study the performance of NCR-assisted networks. More specifically, this paper performs a system level evaluation to analyze the performance improvement that an NCR can cause in its serving cell. Also, we evaluate the effect of the interference that NCRs can have on the neighbor cells.

The rest of the paper is organized as follows. Section II presents the main concepts related to NCR. The scenario considered in the performance evaluation is presented in Section III. Section IV presents the performance evaluation results. Finally, conclusions are presented in Section V.

II. NETWORK CONTROLLED REPEATER

Traditional RF repeaters used in previous generations of wireless communications are non-regenerative nodes that amplify and forward a received signal. A direct consequence of this is the increase of interference in the system [8].

The NCR concept is an evolution of the RF repeaters that use side control information to overcome the negative aspects of traditional repeaters. Side control information that can be used by NCRs are [8]:

- ON/OFF information: turn on/off the amplify and forward on a given slot;
- Timing information: dynamic downlink (DL)/uplink (UL) split;
- Spatial transmitter (Tx)/ receiver (Rx): beamforming capability.

NCR can be split into NCR-mobile termination (MT) and NCR-forwarding (Fwd), as is shown in Fig. 1. The NCR-MT is responsible for exchanging side control information with its

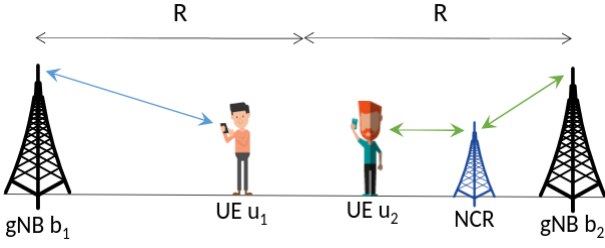


Fig. 2. Scenario with two gNBs (distant $2R$ from each other) and two UEs, connected to different gNBs. Moreover, it is considered that one of the gNBs controls an NCR, which is deployed between its controller gNB and its serving UE.

controlling gNB. Its link is called control link, and it is based on new radio (NR) Uu interface. The NCR-Fwd is responsible for executing the amplify and forward (AF) relaying [7].

III. SYSTEM MODEL

As shown in Fig. 2, consider a scenario with two gNBs, i.e., b_1 and b_2 . The inter-site distance (ISD) between them is equal to $2R$. Also, consider that there is one user equipment (UE) close to each cell edge, i.e., UEs u_1 and u_2 at cells of gNBs b_1 and b_2 , respectively. In the cell of gNB b_2 , an NCR is deployed between b_2 and UE u_2 to enhance the link serving u_2 as shown in Fig. 2.

Since we consider that the UEs are close to the cell edge, the gNB antenna array is deployed such that it steers to the middle point between its respective UE and itself. Furthermore, the NCR backhaul antenna array is always pointing towards the gNB b_2 direction, while its access antenna array points towards the UE u_2 .

Regarding the signal to noise ratio (SNR) and signal to interference-plus-noise ratio (SINR) perceived by the UEs in the DL, their expressions are determined as follows.

Consider a physical resource block (PRB) as the smallest allocable frequency unit, which consists of a number of adjacent subcarriers in the frequency domain. The system bandwidth is split into K PRBs. Moreover, consider that UE u_1 always connects directly to gNB b_1 , while UE u_2 connects to gNB b_2 either directly or through the NCR.

The power received by a node r from a signal that was transmitted by a node t at PRB k , where the pair (t, r) can be, for example, (b_1, u_1) , (b_2, u_2) , (b_2, NCR) , (NCR, u_2) , etc., is expressed as

$$p_{t,r,k}^R = \frac{p_{t,k}^T g_t^T g_r^R}{l_{t,r}}, \quad (1)$$

where $p_{t,k}^T$ is the power transmitted by node t at PRB k , g_t^T is the transmit panel gain of node t , g_r^R is the receive panel gain of node r , and $l_{t,r}$ is the pathloss between nodes t and r . Notice that, for the pairs $(t, r) \in \{(b_1, u_2), (b_2, u_1), (\text{NCR}, u_1)\}$, $p_{t,r,k}^R$ represents an interfering power, while, for the pairs $(t, r) \in \{(b_1, u_1), (b_2, u_2), (b_2, \text{NCR}), (\text{NCR}, u_2)\}$, $p_{t,r,k}^R$ represents the useful power.

When gNB b_2 serves UE u_2 via NCR, the NCR transmit power on PRB k $p_{\text{NCR},k}^T$ is equal to the NCR total receive power, i.e., the sum of the useful power $p_{b_2,\text{NCR},k}^R$, the noise p_n and the interfering power $p_{\text{NCR},k}^I = p_{b_1,\text{NCR},k}^R$, amplified by

a gain g^{NCR} , limited by the NCR maximum transmit power per PRB $p_{\text{MAX}}^{\text{NCR}}$. It can be expressed as

$$p_{\text{NCR},k}^T = \min\{p_{\text{MAX}}^{\text{NCR}}, g^{\text{NCR}}(p_{b_2,\text{NCR},k}^R + p_n + p_{\text{NCR},k}^I)\}. \quad (2)$$

We consider that the NCR gain can be either fixed or dynamic¹. When using the dynamic gain, the NCR transmit power $p_{\text{NCR},k}^T$ is always equal to the NCR maximum transmit power $p_{\text{MAX}}^{\text{NCR}}$. For this, the dynamic gain is defined as the ratio between the NCR maximum transmit power, i.e., $p_{\text{MAX}}^{\text{NCR}}$, and NCR total receive power, i.e., the sum of the useful power $p_{b_2,\text{NCR},k}^R$, the noise p_n and the interfering power $p_{\text{NCR},k}^I = p_{b_1,\text{NCR},k}^R$. We remark that the NCR does not need to know the values of $p_{b_2,\text{NCR},k}^R$, $p_{\text{NCR},k}^I$ and p_n separately. It just need to know their sum, which is known since it is the total input power that it receives. Thus, the dynamic gain can be expressed as

$$g_{\text{DYN}}^{\text{NCR}} = \frac{p_{\text{MAX}}^{\text{NCR}}}{p_{b_2,\text{NCR},k}^R + p_{\text{NCR},k}^I + p_n}. \quad (3)$$

Regarding the fixed gain, i.e., $g_{\text{FIX}}^{\text{NCR}}$, it amplifies the total received power with a fixed value, e.g., 90 dB. When the fixed gain implies an NCR total transmit power higher than its ceiling $p_{\text{MAX}}^{\text{NCR}}$, the NCR works in a saturated mode. In this mode, it behaves similar to the dynamic gain, where the NCR transmit power $p_{\text{NCR},k}^T$ is equal to the NCR maximum transmit power $p_{\text{MAX}}^{\text{NCR}}$.

Thus, the SNR and SINR perceived by UE u_i at PRB k are, respectively, given by

$$\rho_{u_i,k} = \frac{p_{u_i,k}^R}{p_{u_i}^N}, \quad (4)$$

and

$$\eta_{u_i,k} = \frac{p_{u_i,k}^R}{p_{u_i,k}^I + p_{u_i}^N}, \quad (5)$$

where $p_{u_i}^N$ is the receiver noise, $p_{u_i,k}^R$ is the useful power received by u_i at PRB k and $p_{u_i,k}^I$ is the interference suffered by u_i at PRB k .

Regarding $p_{u_i,k}^R$, on the one hand, for u_1 , the only useful signal received is the one coming from b_1 , thus

$$p_{u_1,k}^R = p_{b_1,u_1,k}^R. \quad (6)$$

On the other hand, u_2 may receive two components of useful signal, one coming directly from b_2 and other being amplified and forwarded by the NCR. Thus,

$$\begin{aligned} p_{u_2,k}^R &= p_{b_2,u_2,k}^R + p_{\text{NCR},u_2,k}^R \\ &= \frac{p_{b_2,k}^T g_{b_2}^T g_{u_2}^R}{l_{b_2,u_2}} + \frac{\left(p_{b_2,\text{NCR},k}^R g^{\text{NCR}}\right) g_{\text{NCR}}^T g_{u_2}^R}{l_{\text{NCR},u_2}} \\ &= \frac{p_{b_2,k}^T g_{b_2}^T g_{u_2}^R}{l_{b_2,u_2}} + \frac{\left(\frac{p_{b_2,k}^T g_{b_2}^T g_{\text{NCR}}^R}{l_{b_2,\text{NCR}}}\right) g^{\text{NCR}} g_{\text{NCR}}^T g_{u_2}^R}{l_{\text{NCR},u_2}} \\ &= \frac{p_{b_2,k}^T g_{b_2}^T g_{u_2}^R}{l_{b_2,u_2}} + \frac{p_{b_2,k}^T g_{b_2}^T g_{\text{NCR}}^T g^{\text{NCR}} g_{\text{NCR}}^T g_{u_2}^R}{l_{b_2,\text{NCR}} l_{\text{NCR},u_2}}. \quad (7) \end{aligned}$$

¹Only NCR fixed gain has been specified by the 3GPP. So, while we try to mimic the model specified by 3GPP Rel-18, the considered setup may have differences with Rel-18 NCR.

TABLE I
CHARACTERISTIC OF THE LINKS

Link	Scenario	LOS/NLOS
gNB - UE	Urban Macro	NLOS
gNB - NCR	Urban Macro	NLOS
NCR - UE	Urban Micro	LOS

Concerning $p_{u_i,k}^I$, with NCR, there are two sources of interference for u_i , which are the signal from b_j , with $i \neq j$, and this same signal amplified by the NCR, thus

$$p_{u_i,k}^I = \frac{p_{b_j,k}^T g_{b_j}^T g_{u_i}^R}{l_{b_j,u_i}} + \frac{p_{b_j,k}^T g_{b_j}^T g_{NCR}^R g_{NCR}^T g_{u_i}^R}{l_{b_j,NCR} l_{NCR,u_i}}. \quad (8)$$

Finally, similarly to what has already been presented, regarding $p_{u_i}^N$, we have

$$p_{u_1}^N = p_n \quad (9)$$

$$p_{u_2}^N = p_n \left(1 + \frac{g_{NCR}^T g_{NCR}^R g_{u_2}^R}{l_{NCR,u_2}} \right). \quad (10)$$

IV. PERFORMANCE EVALUATION

A. Simulation Assumptions

The simulations were conducted at 28 GHz. The frequency domain was split into PRBs consisting of 12 consecutive subcarriers, with subcarrier spacing of 60 kHz. It was adopted the round robin (RR) scheduler for allocating the PRBs.

Concerning the time domain, it was split into slots composed of 14 orthogonal frequency division multiplexing (OFDM) symbols. Each slot had a duration of 0.25 ms. A time division duplex (TDD) scheme was adopted, where downlink and uplink slots were alternated in time.

Regarding the channel model, the adopted one is based on the 3GPP channel model standardized in [9] and its implementation is described in [10]. In this channel model, it is considered a distance-dependent pathloss, a lognormal shadowing component, a small-scale fading, and it is spatially and time consistent. The link types are described in Table I. The gNBs and the NCR transmissions were performed with a discrete fourier transform (DFT) codebook based beamforming, where for each transmission a beam management was performed in order to identify the best transmitter beam to be used when serving the UEs.

It was used a channel quality indicator (CQI)/modulation and coding scheme (MCS) mapping curve standardized in [11] with a target block error rate (BLER) of 10 %. An outer loop strategy was considered to avoid the increase of the BLER, i.e., when a transmission error occurred, the estimated SINR decreased 1 dB, however, when a transmission occurred without error, the estimated SINR had its value added by 0.1 dB. The most relevant simulation parameters are summarized in Tables II and III.

B. Simulation Results

Figures 3 and 4 show the impact of NCR position on the SNR (quantiles 0.9 and 0.1, respectively) of UEs u_1 and u_2 . Both figures present the results for the two possibilities of the NCR gain: dynamic and fixed. For the fixed case, we considered two gain values: 70 dB and 90 dB. Considering the positions of u_2 and b_2 fixed, the x-axis represents the possible distance

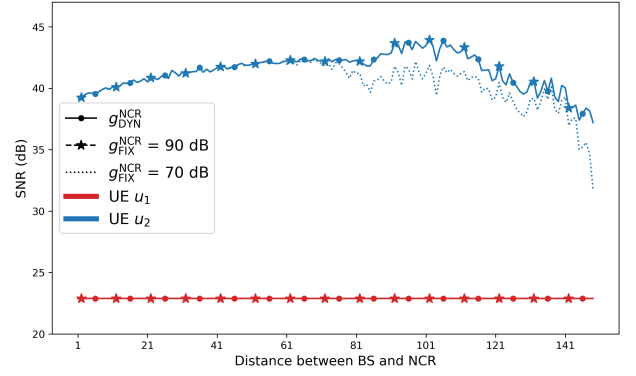


Fig. 3. Impact of NCR position on the SNR (quantile 90%) of both UEs for two types of NCR gain, i.e., dynamic and fixed.

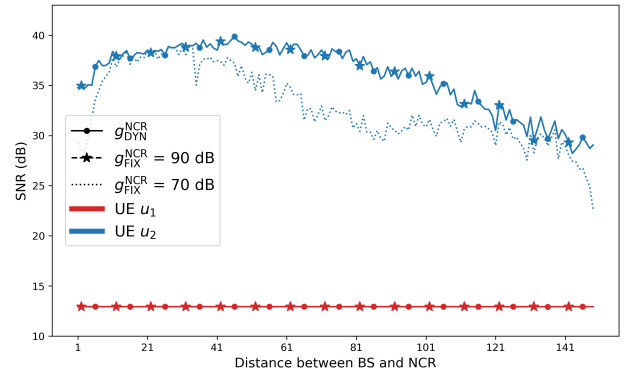


Fig. 4. Impact of NCR position on the SNR (quantile 10%) of both UEs for two types of NCR gain, i.e., dynamic and fixed.

between the NCR and b_2 . As expected, the SNR of u_1 does not depend of the position of the NCR. Also, notice that the SNR of u_2 , in the beginning, increases and, after a certain distance, starts to decrease. This is due to the product of the two pathlosses in (7), i.e., $l_{b_2,NCR} l_{NCR,u_2}$. Thus, unlike what one could expect, deploying a NCR closer to the serving UE does not always mean a better connection. In other words, one could expect that the closer a UE is to a NCR the higher its SNR would be due to the shorter distance, and so lower path loss, however as shown in Figs. 3 and 4, this is not true.

Due to the symmetry of the scenario presented in Fig. 2, without the NCR, u_1 and u_2 should present similar values of SNR and SINR. Thus, by comparing the curves in Fig. 3 and Fig. 4 related to u_1 and u_2 , we can see that the deployment of an NCR considerably improves the SNR perceived by u_2 . More specifically, the SNR perceived by u_2 increased in at least 15 dB due to the deployment of the NCR. Moreover, notice that the case with fixed NCR gain equal to 90 dB presented results similar to the dynamic case, which means that for 90 dB, the NCR operated in its saturated mode.

Figures 5 and 6 are similar to Figs. 3 and 4, the main difference is that Figs. 5 and 6 focus on SINR instead of SNR.

Notice, in Figs. 5 and 6, the trend discontinuity on the SINR of u_1 when the distance between the NCR and b_2 is approximately 81 m. This is explained by the change in the interference coming from the NCR. More specifically, around that distance the beam used by the NCR to serve u_2 changes creating a new interference pattern on u_1 . Fig. 7 illustrates

TABLE II
ENTITIES CHARACTERISTICS.

Parameter	Macro gNB	NCR	UE
Height	25 m	10 m	1.5 m
Transmit power	16.8 dBm	13.8 dBm	5.8 dBm
Antenna array	URA 8×8	URA 8×8 (2 panels)	Single Antenna
Antenna element pattern	3GPP 3D [9]	3GPP 3D [9]	Omni
Max. antenna element gain	8 dBi	8 dBi	0 dBi

TABLE III
SIMULATION PARAMETERS.

Parameter	Value
Carrier frequency	28 GHz
Subcarrier spacing	60 kHz
Number of subcarriers per RB	12
Number of RBs	1
Slot duration	0.25 ms
OFDM symbols per slot	14
Channel generation procedure	As described in [9, Fig.7.6.4-1]
Path loss	Eqs. in [9, Table 7.4.1-1]
Fast fading	As described in [9, Sec.7.5] and [9, Table 7.5-6]
AWGN density power per subcarrier	-174 dBm/Hz
Noise figure	9 dB
CBR packet size	3072 bits
Inter-site distance	400 m
Distance between gNB and UE	150 m

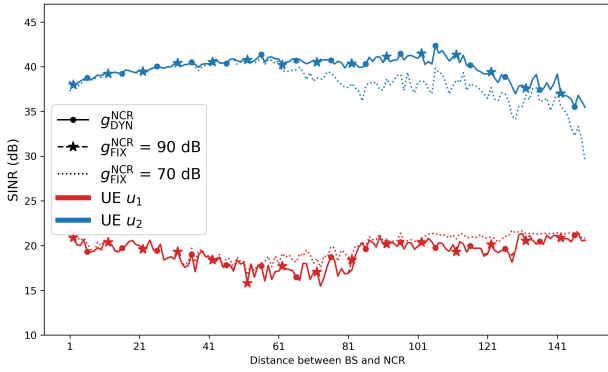


Fig. 5. Impact of NCR position on the SINR (quantile 90%) of both UEs for two types of NCR gain, i.e., dynamic and fixed.

this behavior.

Fig. 7 presents the impact of the distance between b_2 and the NCR on the interference suffered by u_1 (y-axis of left-hand side) and on the beam index that is used to serve u_2 (y-axis of right-hand side). In this figure, we can notice that the interference suffered by u_1 has a discontinuity when the distance between b_2 and the NCR is around 81 m. Around this position, the NCR beam serving u_2 changes from 0 to 1. Beam 0 points in a direction closer to u_1 than Beam 1, that is why when changing from Beam 0 to Beam 1, the interference decreases. This can be seen as a spatial filtering.

Furthermore, notice, in Fig. 7, that within the distance ranges 0 m to 81 m and 81 m to 150 m, the interference suffered by u_1 increases when the NCR distance between b_2 and the NCR increases. This is explained by the approximation of the NCR to u_1 .

Finally, Figs. 8 and 9 present the impact of the distance between b_2 and the NCR on the spectral efficiency of the transmissions to u_1 and u_2 . The maximum spectral efficiency

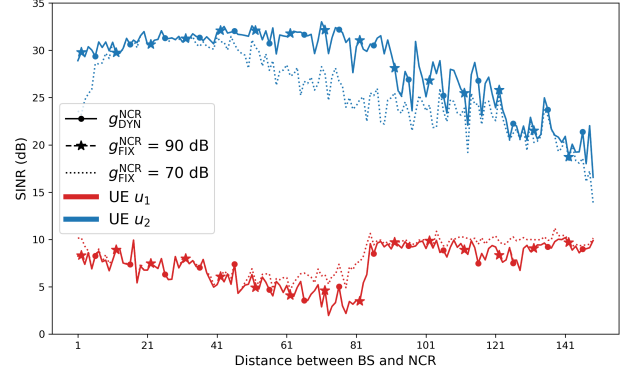


Fig. 6. Impact of NCR position on the SINR (quantile 10%) of both UEs for two types of NCR gain, i.e., dynamic and fixed.

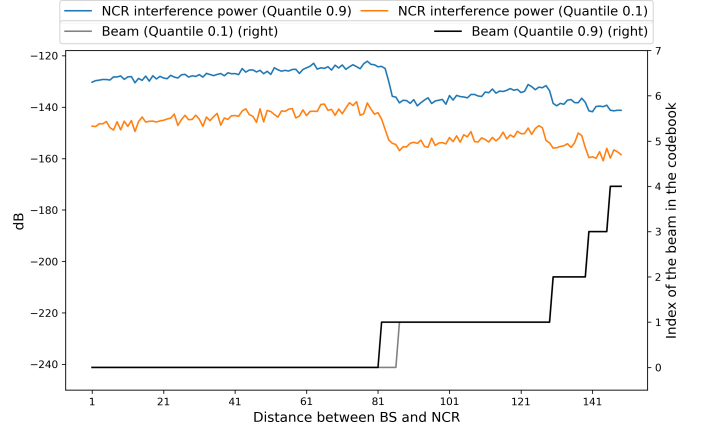


Fig. 7. Comparison between the interference and amplified noise by NCR in the u_1 and the change in the codebook indexes of the NCR-Fwd.

that a transmission could achieve is:

$$\frac{\text{subcarriers per PRB} \cdot \text{symbols per PRB} \cdot \text{max. code rate}}{\text{PRB time} \cdot \text{PRB bandwidth}} = \frac{12 \cdot 14 \cdot 5.5547}{0.25 \cdot 10^{-3} \cdot 12 \cdot 60 \cdot 10^3} = 5.18 \text{ bits/s/Hz}, \quad (11)$$

where 5.5547 corresponds to the code rate associated to the CQI index 15 in [11]. Remark that u_2 achieves the maximum spectral efficiency in the majority of the considered cases, while u_1 achieves lower values, but that are still high enough to allow the communication.

V. CONCLUSIONS

The paper presented a system level evaluation analyzing the performance improvement due to the deployment of a NCR on a given cell and its interference impact on neighbor cells. As expected, we have seen that the NCR improves the link quality of its serving UE. However, unlike what one could expect, deploying a NCR closer to its serving UE does not necessarily mean a better connection. There is a trade-off given

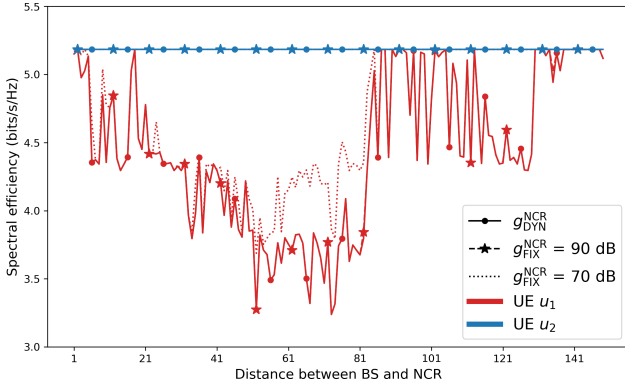


Fig. 8. Spectral efficiency (quantile 90%) of the both UEs and with different types of NCR gain.

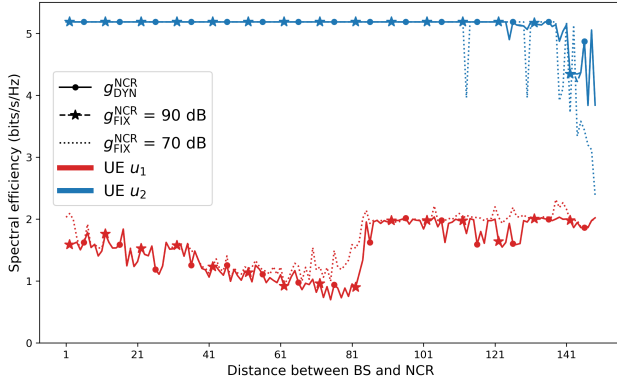


Fig. 9. Spectral efficiency (quantile 10%) of the both UEs and with different types of NCR gain.

by the product between its distance to its serving gNB and its distance to the UE that it is serving. We have also seen that the interference caused on neighbor cells can be mitigated by spatial filtering by means of appropriate beam management.

REFERENCES

- [1] K. Dong, S. Mura, M. Mizmizi, D. Tagliaferri, and U. Spagnolini. "Advanced tri-sectoral multi-user millimeter-wave smart repeater." arXiv: 2210.04859. (Oct. 2022).
- [2] R. Flamini, D. De Donno, J. Gambini, *et al.*, "Towards a heterogeneous smart electromagnetic environment for millimeter-wave communications: An industrial viewpoint," *IEEE Trans. Antennas Propag.*, vol. 70, no. 10, pp. 8898–8910, Feb. 2022. DOI: 10.1109/TAP.2022.3151978.
- [3] M. Polese, M. Giordani, T. Zugno, *et al.*, "Integrated access and backhaul in 5G mmWave networks: Potential and challenges," *IEEE Commun. Mag.*, vol. 58, no. 3, pp. 62–68, Mar. 2020. DOI: 10.1109/MCOM.001.1900346.
- [4] R. A. Ayoubi, M. Mizmizi, D. Tagliaferri, D. D. Donno, and U. Spagnolini. "Network-controlled repeaters vs. reconfigurable intelligent surfaces for 6G mmW coverage extension." arXiv: 2211.08033. (Nov. 2022).
- [5] C. Madapatha, B. Makki, C. Fang, *et al.*, "On integrated access and backhaul networks: Current status and potentials," *IEEE Open J. Commu. Soc.*, vol. 1, pp. 1374–1389, Sep. 2020. DOI: 10.1109/OJCOMS.2020.3022529.
- [6] H. Guo, C. Madapatha, B. Makki, *et al.* "A comparison between network-controlled repeaters and reconfigurable intelligent surfaces." arXiv: 2211.06974. (Nov. 2022).
- [7] 3GPP, "Study on NR network-controlled repeaters: Radio Interface Protocol Aspects," 3rd Generation Partnership Project (3GPP), TR 38.867, Sep. 2022, v.18.0.0.
- [8] *Rws-210019: Nr smart repeaters*, Qualcomm, 2021.

- [9] 3GPP, "Study on channel model for frequencies from 0.5 to 100 GHz," 3rd Generation Partnership Project (3GPP), TR 38.901, Sep. 2017, v.14.2.0.
- [10] A. M. Pessoa, I. M. Guerreiro, C. F. M. e Silva, *et al.*, "A stochastic channel model with dual mobility for 5G massive networks," *IEEE Access*, vol. 7, pp. 149971–149987, Oct. 2019, ISSN: 2169-3536. DOI: 10.1109/ACCESS.2019.2947407.
- [11] 3GPP, "NR; physical layer procedures for data," 3rd Generation Partnership Project (3GPP), TS 38.214, Dec. 2017, v.15.0.0.